Desalination 583 (2024) 117693

Contents lists available at ScienceDirect

Desalination

journal homepage: www.elsevier.com/locate/desal

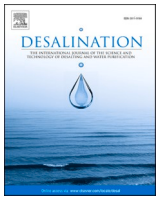

Polyelectrolyte multilayer membranes: An experimental review

Jurjen A. Regenspurg, Wendy A. Jonkers, Moritz A. Junker, Iske Achterhuis, Esra te Brinke, Wiebe M. de Vos *

Twente Membranes, University of Twente, MESA+ Institute for Nanotechnology, P.O. Box 217, 7500 AE, Enschede, the Netherlands

ARTICLE INFO

Keywords:
Nanofiltration
Hollow fiber
Reverse osmosis
Membrane production
Coating

ABSTRACT

Within just two decades, polyelectrolyte multilayer (PEM) membranes have moved from invention to their world wide application. One key advantage of these membranes is their versatility, allowing easy optimization through various tuning parameters. But it is exactly this versatility that has made it difficult to fairly compare PEM membranes. Previously, only Krasemann and Tieke (2000) have compared a large set polyelectrolyte pairs for their membrane performance, concluding that the polyelectrolyte charge density was a key tuning parameter. However, in these early days of PEM membrane research, characterization was rather limited. In this work, we have performed a thorough experimental review, studying 9 common polyelectrolyte pairs for their layer properties on model surfaces and their separation properties as pressure driven membranes. All systems were prepared under identical conditions to allow for a fair comparison, and membranes were characterized for their water permeability, molecular weight cut off, and ion retention. We find that the porous support is closed by a PEM when its thickness is in the order of the membrane support pore size, which was expected but not demonstrated before. Of all the PEM parameters, the degree of swelling stands out as a parameter that plays a key role and can be easily experimentally determined. Interestingly, we find that swelling increases with polyelectrolyte charge density, which is opposite to what Krasemann and Tieke proposed. We attribute this to the higher hydrophilicity of polyelectrolytes with a higher charge density. In turn, we find correlations between swelling and the water permeability as well as size exclusion, dielectric exclusion and Donnan exclusion. Still, the connection between polyelectrolyte properties and membrane properties is more complex and cannot be solely understood by swelling. Further understanding of this complexity will provide the tools to develop even better polyelectrolyte multilayer membranes.

1. Introduction

Polyelectrolyte multilayer (PEM) based separation membranes can certainly be seen as a recent scientific success story, strongly connecting the fields of colloid and interface science and membrane science. What started a little >30 years ago, with the first paper on PEMs by Decher and co-workers [1], has by now evolved into a membrane technology that provides many millions of litres of clean drinking water per day and that number is rapidly growing [2].

Looking back now, we can distinguish roughly 3 periods. After the first paper of Decher and co-workers in 1991, the focus was initially on the fundamental aspects of the PEM formation [3–5], but also on the preparation of multilayers with many different components, including not just various polycation and polyanion pairs [6], but also charged nano particles [7], nucleotides [8], dendrimers [9] and protein molecules [10]. Still even in these early days, the Layer-by-Layer (LbL) concept was considered for applications, for example as capsules for drug delivery as made popular by the group of Mohwald [11], or as sensor [12] or anti-fouling coating [13]. Even the use of PEMs for gas separation membranes was already proposed and tried out, although not with great success [14].

The focus on PEMs for membranes in water treatment started in 2000 with the work of especially Krasemann and Tieke [15], quickly followed by work from the group of Bruening [16]. Both groups clearly showed the promise of using PEM based membranes for the retention of ions from water. In the years following this breakthrough, a lot of progress was made. PEMs were used to provide many different functionalities to membranes, including membranes for protein retention/adsorption [17], (bio)catalytic membranes [18] and for separations ranging from ultrafiltration [19] and nanofiltration [20] to reverse osmosis [21].

* Corresponding author.
E-mail address: w.m.devos@utwente.nl (W.M. de Vos).

https://doi.org/10.1016/j.desal.2024.117693
Received 26 January 2024; Received in revised form 15 April 2024; Accepted 24 April 2024
Available online 1 May 2024

Especially the group of Bruening pioneered the use of PEM coatings to achieve ionic selectivity in electrically driven membrane processes [22,23].

Then in more recent years, the field started to converge towards hollow fiber nanofiltration membranes, showing very clear advantages in comparison with the commercial spiral wound membranes based on interfacial polymerization [2,24,25]. With PEMs it is easy to prepare a hollow fiber membrane, either through dynamic coating [26] or dip-coating [27], whereas with interfacial polymerization this is very difficult [28]. Moreover, the chemical stability of especially PDADMAC/PSS provides these membranes with an unprecedented resistance against the essential chemical cleaning steps that need to be regularly applied in membrane processes [29–31]. Together this allows the direct use of nanofiltration even in very highly polluted streams such as municipal wastewater, where previously always a pre-treatment by for example a UF membrane was needed to utilize an NF membrane [2,24,32]. These advantages led to commercialization of the approach by companies like Pentair X-flow and NX Filtration, who now sell these membranes on a worldwide scale [2].

Apart from the advantages above, one of the key advantages of LbL based membranes is thought to be their very high versatility [33,34]. As mentioned widely varying separation properties, ranging from UF to RO can be achieved by careful tuning of the coating conditions (such as the ionic strength [35], ion type [36], pH [37], polyelectrolyte (PE) Mw [38]), the chosen polyelectrolytes [15,39], the choice of support membrane [40] and the use of post treatment such as annealing [41] or crosslinking [42]. Utilizing these parameters, PEM based membranes can really be optimized towards a given feed and given separation case to separate based on unique combinations of size, Donnan and/or dielectric based exclusion [33,34].

But strangely enough, that versatility can also be considered a challenge. With so many scientists preparing PEM based membranes under different conditions and on different membrane supports, as well as measuring their performance under different process conditions, it becomes very difficult to fairly compare different PEM based membranes. Especially the effect of the exact type of polyelectrolyte is an aspect where no clear fundamental understanding has been reached. Remarkably, the most complete work on this topic, comparing different PEM systems, is the original work of Krasemann and Tieke [15], where they compared 8 different PEM systems, and measured the resulting permeability of different salt ions. In this highly influential manuscript they introduced the concept of polyelectrolyte charge density to explain the trends that they observed. For monomers with a higher charge density, here defined as couple of cationic and anionic monomer per number of carbon atoms, a denser membrane would be expected due to a higher degree of ionic crosslinks per unit of volume. And indeed, the authors found a clear decreasing trend, with a higher charge density leading to a lower salt permeance (see Fig. 1). This work is the only publication so far that provides a comparison of a larger number of polyelectrolyte pairs. While other studies sometimes also looked at different PEM systems, their scope was always much smaller, typically limited to the comparison of just 2–3 PEM combinations [39,43–45].

But with the many new insights that we have gained in the past two decades, we also need to acknowledge that the study of Krasemann and Tieke had limitations. For example, every system was coated for exactly 60 bilayers, but for different PEM systems layer growth can vary wildly. Indeed, the difference between a linear growing systems such as PAH/PSS and an exponentially growing system like PAH/PAA can easily reach a difference in thickness (after 5–7 bilayers) of a factor 5–10 [38]. Such significant differences in thickness will affect permeation rates. Moreover, salt permeance is by itself not such a relevant parameter for membrane separations, if the water permeability is not known. For example, a membrane that blocks all salt, but also all water is still not a useful membrane. Finally, ion transport is strongly governed by ionic interactions, and gives limited prediction for the effective pore size (or molecular weight cut off, MWCO), which is a key parameter to describe the mechanism of size exclusion in a membrane separation [46].

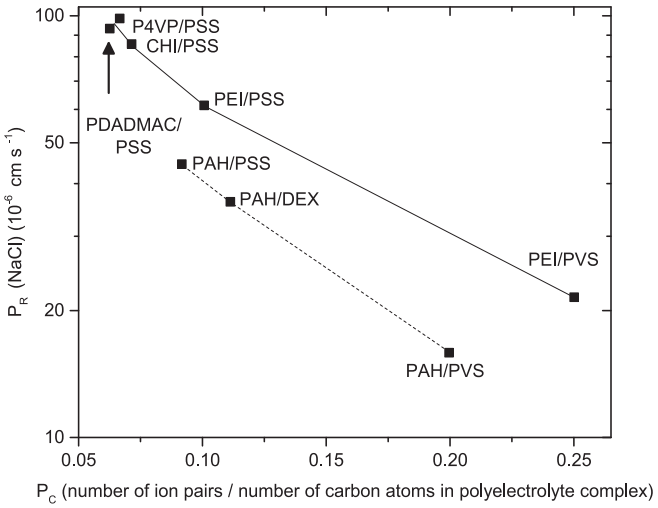

Fig. 1. A key figure from the work of Krasemann and Tieke (2000) [15], showing the salt permeance as function of the charge density for 8 different PEM systems. All PEM coatings were 60 bilayers in thickness, while the salt permeance was measured under diffusion.

In this work, we build on the work of Tieke and Krasemann to fairly compare 9 different polyelectrolyte systems. These systems were selected as they represent the 9 most studied PEM systems for membrane application. For all systems, the PEM coatings were studied on model surfaces, for their thickness and degree of hydration, and as membrane coatings for their pure water permeance, MWCO and for the rejection of various ions (NaCl, $MgCl_2$, Na_2SO_4 and $MgSO_4$). To fairly compare the membrane thickness, we measured the performance for membranes comprised of different numbers of bilayers to accurately determine the minimum number of layers that effectively closes the support pores and thus dominates the membrane transport.

2. Materials and methods

2.1. Materials

Poly(vinylsulfuric acid potassium salt) (PVS, $M_w = 175{,}000$ g·mol^{-1}) was purchased from Fisher Scientific™. Poly(sodium 4-styrenesulfonate) (PSS, M_w = 200,000 g·mol^{-1}, 30 wt% in H_2O), Poly(acrylic acid) (PAA, M_w = 250,000 g·mol^{-1}, 35 wt% in H_2O), Poly(diallyl dimethylammonium chloride) (PDADMAC, M_w = 200,000–350,000 g·mol^{-1}, 20 wt% in H_2O), Chitosan (CHI, medium molecular weight, 85 % deacetylated) and Poly(ethylenimine) (PEI, M_w = 25,000 g·mol^{-1}, branched) were obtained from Sigma Aldrich. Poly(allylamine hydrochloric acid) (PAH, M_w = 150,000 g·mol^{-1}, 40 wt% in H_2O) was obtained from Nittobo medical CO., LTD, Japan. Poly(vinylamine) (PVA, M_w = approximately 400, 000 g·mol^{-1}, 16–18 % in H_2O) was kindly provided by BASF. $MgCl_2$ hexahydrate (purity 99 %) was purchased from Sigma Aldrich, NaCl (purity 99.9 wt%) was kindly provided by Nouryon industrial chemicals. Na_2SO_4 decahydrate was obtained from Merck. Ethylene glycol and polyethylene glycol (PEG) of various M_w (200, 400, 600 and 1000 Da) were purchased from Merck. Diethylene glycol was purchased from Sigma Aldrich. H_2O_2 (30 *w*/w% solution in H_2O) was obtained from Merck. H_2SO_4 (96 % in H_2O) was purchased from Acros organics B.V.B.A Sodium hydroxide (pellets, purity 98 %) and hydrochloric acid (ACS reagent, 37 %) were purchased from Sigma Aldrich. Glycerol solution (86–89 %) was purchased from Sigma Aldrich. Modified poly(ether sulfone) HF UF membranes were kindly provided by NX Filtration B.V., Enschede, the Netherlands. The provided membranes have an inner diameter of 0.7 mm and approximate 90 % MWCO of 10 kDa. All Chemicals were used without any further

purification.

2.2. Methods

Choice of polyelectrolytes - An indication of how much has been published on each polyelectrolyte pair was generated by writing down the number of hits for each polyelectrolyte pair in the Scopus database. For this, we searched in the Article title, Abstract, Keywords for the keywords: *'polycation AND polyanion AND multilayer AND membrane'* on 14-12-2023.

Membrane fabrication - HF PEM membranes were fabricated by means of dip coating. Modified poly(ether sulfone) HF UF membranes, with a negative surface charge, were used as substrates for PEM deposition. Dip coating was performed in cycles consisting of coating and washing steps. Coating steps were performed using aqueous PE solutions prepared with 50 mM NaCl and 0.1 g/L, either anionic or cationic, PE set to a pH of 5.5. Rinsing steps were performed with an aqueous 50 mM NaCl solution. To complete a full cycle, support membranes were immersed into a poly-cation solution for 15 min for a so-called coating step. After the coating step the support membranes are subsequently immersed into 3 separate rinsing solutions for 5 min each to remove loosely bound PEs. Sequentially, the support membranes are submersed into a poly-anion solution for 15 min. This cycle can be repeated until the desired amount of bilayers is reached upon which the membranes are rinsed twice for 5 min each using the before mentioned rinsing solutions. The desired amount of bilayers is determined by means of growth curves (Fig. S3).

After dipcoating, the HF PEM membranes are immersed into a 15 wt % glycerol solution for 4 h to prevent pores collapsing upon drying overnight. After drying, hollow fibers were glued into plastic tubing (6 mm outer diameter) with the use of a 2-component polyurethane glue. Permeate was collected via a hole at the midpoint of the plastic tubing (Fig. S1).

Ellipsometry - Dry and wet multilayer thickness was determined by means of ellipsometry (rotating compensator ellipsometer Mk-2000 V and Mk-2000 X, J.A. Woollam Co., Inc.). Experiments were performed on model surfaces following the method described by Junker et al. [46], except that neutral pH conditions (pH = 7) were applied in the current work. All prepared and measured multilayers were ending on a negatively charged polyelectrolyte layer and consisted of 10 bilayers (note: this only holds for ellipsometry measurements). Using eq. 1 the swelling ratio (SR) was calculated.

$$SR = \frac{d_{wet} - d_{dry}}{d_{dry}} \bullet 100\% \tag{1}$$

Reflectometry - By means of fixed angle reflectometry the amount of adsorbed polymer was monitored in-situ. A silicon wafer with a layer of silicon oxide (82 nm) was placed into a stagnation pint flow cell. Subsequently, the silicon wafer was alternately exposed to polycation and polyanion (0.1 g/L in 50 mM aqueous NaCl solution at pH 5.5). A linearly polarized monochromatic light beam (He—Ne laser; 632.8 nm) is reflected of the surface under the Brewster angle resulting in P- and S-polarized components. Due to the changing amount of adsorbed polyelectrolyte the intensities of both components change, eq. 2 allows us to calculate the adsorbed amount of polyelectrolyte. The used setup and method are elaborately described by Dijt et al. [47]

$$\Gamma = Q \bullet \frac{\Delta S}{S_0} \tag{2}$$

In eq. 2, (Γ) is the amount of adsorbed polymer in mg/m^2. By taking the ratio between intensities of both P and S components we derive S_0. ΔS represents the change in intensity ratio upon adsorption of polyelectrolyte to the model surface. Q is the sensitivity factor, also known as Q-factor, and is derived using an optical model. This model makes use of the refractive indexes (n), refractive index increment (dn/dc) of both polyelectrolytes, silicon oxide layer thickness, adsorbed layer thickness (d) as well as the angle of incidence ($\theta = 71^\circ$). The Q-factor for each polyelectrolyte was calculated using the following values: $n_{silica} = 1.46$, $n\sim_{silicon} = (3.85, 0.02)$, $n_{H2O} = 1.33$. dn/dc values were determined for all the used PEs by means of refractometry using a Schmidt+Haensch ATR-L spectral refractometer at wavelengths of 590 and 700 nm. The obtained dn/dc values and resulting Q-factors are displayed in Table S1.

Membrane performance - The performance of the prepared membranes was determined in terms of pure water permeability, charged solute retention and uncharged solute retention. All experiments were conducted in a crossflow configuration (Fig. S2) at a constant transmembrane pressure of 2 bar, a cross-flow velocity of 1 ms^{-1} while controlling feed temperature at 20 ± 0.5 °C.

Pure water permeability experiments were performed using Milli-Q water. Permeate was collected over time and weighed. Using eq. 3 the pure water permeability (Lm^{-2}h^{-1}bar^{-1}) was calculated.

$$Permeability = \frac{M_p}{\rho_w \bullet A \bullet t \bullet \Delta P} \tag{3}$$

The collected permeate mass is defined as m_p in g, ρ_w equals the density of water (1000 gL^{-1} at 20 °C), A is the active membrane area in m^2, t is the duration of the experiment in h and ΔP is the transmembrane pressure in bar.

To determine the overall charge of the PEM membranes charged solute retention experiments were performed. For this purpose the following salts were used; NaCl, $MgCl_2$, Na_2SO_4 and $MgSO_4$. Single salt solutions were prepared using Milli-Q water with salt concentrations of 5 mM. By making use of monovalent and divalent salts more insight is obtained with regard to overall membrane charge and retention mechanisms.

$$Salt\ retention = \left(1 - \frac{C_p}{C_f}\right) \bullet 100\% \tag{4}$$

The charged solute retention (%) is calculated using eq. 4 by making use of conductivity. Here c_f is the average conductivity of the feed solution between the start and end of the experiment. c_p is the conductivity of the collected permeate sample at the end of the experiment. Conductivity values were obtained using a WTW ProfiLine portable conductivity meter.

To compare the different PEM membrane systems, intrinsic properties (i.e. pure water permeability A (mPa^{-1} s^{-1}) and salt permeability B (ms^{-1})) that are independent of process parameters, such as flux, were determined. The intrinsic membrane properties are calculated based on theoretical transport models commonly applied for pressure driven filtration using dense membranes (i.e. RO and NF), namely the Solution-Diffusion model combined with the Film model (to account for concentration polarisation effects) [48]. More details on the calculation of the A and B parameters can be found in the Supplementary Information (S11).

Uncharged solute retention experiments in the form of molecular weight cut off (MWCO) measurements were performed. The 90 % MWCO allows us to compare the relative differences in pore size between the different PEM membranes. As uncharged solutes a mixture of ethylene glycol, diethylene glycol and various sizes (200-1000 Da) of polyethylene glycol (PEG) were used. The concentration used for each PEG was 1 gL^{-1}. Feed samples were taken at the start and end of every experiment to determine the average signal intensity. Permeate samples were taken at the end of every experiment. All samples were analyzed using gel permeation chromatography (GPC, Agilent 1200/1260 Infinity GPC/SEC series). The GPC was set up with two columns in series obtained from Polymer Standards Service GmbH. The columns; Suprema 8 × 300 mm - 1000°A, 10 μm followed by 30°A, 10 μm were operated at a flow of 1 mL·min-1. The GPC is fitted with a refractive index detector.

3. Results and discussion

Over the years, many different polyelectrolytes have been used for the fabrication of polyelectrolyte multilayers. In this experimental review, 9 polyelectrolyte pairs were selected for comparison. They were selected based on the number of published papers on these pairs, the commercial availability of the polyelectrolytes, and a preference for a wide range of different properties to obtain a representative dataset. Six of the eight polyelectrolytes used by Tieke and Krasemann were included in this selection. The structures of the polyelectrolytes used in this manuscript are displayed in Fig. 2. The selected polyelectrolytes contain a wide range of functional groups and properties, which are provided in more detail in Supporting information Table S2.

For the polyanions, the charge is introduced via either a sulfonate group or a carboxylic acid group. PSS and PVS both contain a sulfonate group. Whereas PSS contains a relatively bulky aromatic group, PVS is much smaller. For PAA charge is introduced by a carboxylic acid group.

For the polycations, the charge is introduced by via the nitrogen atom. Here, the distinction can be made between primary, secondary, tertiary, and quaternary nitrogen atoms. PVA and PAH contain only primary nitrogen groups and look structurally similar, except for a one carbon atom difference. CHI, a polysaccharide, is the only natural compound and contains primary nitrogen groups as well. PEI stands out as it has a combination of primary, secondary, and tertiary nitrogen groups and is the only branched compound. PDADMAC contains a quaternary nitrogen group.

An indication of the number of published papers on each polyelectrolyte pair is given in Table 1. It should be noted that not all hits represent actual papers on the discussed polyelectrolyte pair, and some papers may not be included with the used search terms. However, it does give a rough indication of which PE pairs are used more and less frequently. This also shows that the PE pairs discussed in this paper cover a range from well-established pairs (PAH/PSS, PAH/PAA, PDADMAC/PSS) to pairs that are relatively unknown for the preparation of LbL membranes (CHI/PSS, PVA/PVS, PVA/PSS, PAH/PVS). This means that the amount of available information per pair varies wildly. A short summary of the properties and applications of these polyelectrolyte pairs in LbL membranes is given as well.

To give a clear overview of the very large amount of data underlying this manuscript, the results and discussion section was carefully split in 5 parts: 1. Layer growth and swelling on model surfaces, 2. layer growth on support membranes, 3. water permeability, 4. retention of neutral molecules and 5. retention of ions. In the work we will reflect on the main hypothesis of Krasemann and Tieke [15], where the charge density of the used polyelectrolytes was proposed as critical to the resulting separation properties, with higher charge densities leading to denser and thus more selective coatings. However, we will also propose alternative explanations focusing on the hydration or swelling of the PEM as an essential property that can affect both the transport of charged and neutral species, in line with results from Miller and Bruening [45]. If not indicated differently data is obtained with negatively ending

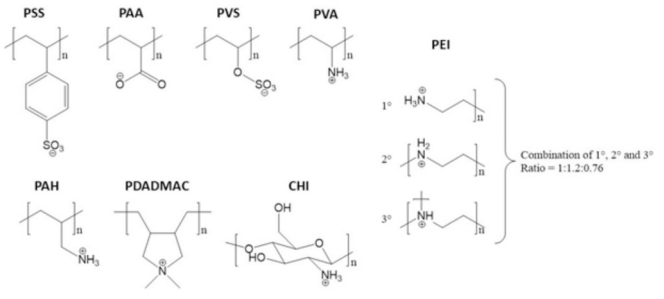

Fig. 2. Structural formulas of the polyelectrolytes used in this study. Polyelectrolytes are displayed in charged form.

Table 1
. Polyelectrolyte pairs used in this study, the number of hits for these pairs in the Scopus database and associated membrane properties.

Polyelectrolyte pair	Scopus hits	Most important properties and applications of multilayer membranes
CHI/PSS	10	CHI/PSS is an interesting system as it incorporates the use of the bio-based amino polysaccharide chitosan. The polymer layer was found to be thermally stable up to 210 °C [49]. This system has mainly been used in niche membrane applications, including the separation of proteins [19] and amino acids [50] and treatment of industrial effluent [51], though the separation efficiency for these streams was found to be highly pH dependent and was mostly attributed to adsorption rather than rejection.
PAH/PSS	88	PAH/PSS is a widely studied system that is stable under acidic conditions [31], and the separation properties are relatively stable when the feed solution pH is modified [46]. Because of its relatively high density [52] but at the same time relatively high water permeability [53], it has been used both as a (crosslinked) top section and as a bottom section in asymmetric PEM membranes [54–56].
PEI/PSS	36	With PEI/PSS, multilayers with a low MWCO can be created [43]. The pair was even used as a gutter layer combined with interfacial polymerization, and this allowed for making hollow fiber RO membranes [28]. A range of different deposition methods has been explored successfully for this pair, including, dip-coating [43], spin-coating [57] and, in combination with carbon nanotubes, inkjet printing [58].
PVA/PSS	5	To the best of our knowledge, only one paper has been published focusing on the use of PVA/PSS in layer-by-layer membranes [59]. Even here, PVA/PSS was merely used as a control membrane for calixarene/PSS membranes. This leaves the use of this system in multilayer membranes severely unexplored.
PDADMAC/PSS	50	PDADMAC/PSS is a well-documented system, known for its excellent stability against the cleaning agent hypochlorite [29], and extreme pH conditions [31]. This can be attributed to both polyelectrolytes bearing permanent charges. Overcompensation of PDADMAC is common in this pair [60].
PVA/PVS	7	The use of PVA/PVS has mostly been limited to a series of works by Toutianoush et al. in the early 2000's. [61–64] Principally, the use of these membranes for the pervaporation separation of ethanol/water mixtures was explored. Compared to other polyelectrolyte pairs which were studied, this pair performed well, which was attributed to the low charge density of this pair.
PEI/PAA	35	PEI/PAA has mainly been used for pervaporation membranes [65] and oxygen barriers [66]. Applications in nanofiltration have been mentioned [67,68], but are much scarcer. Further modification of these layers has been explored, such as the use of glutaraldehyde to crosslink the layers. [67,68]
PAH/PAA	53	PAH/PAA has extensively been used in nanofiltration applications [37,46,54,69]. The use of two weak polyelectrolytes has been known to make the system highly sensitive to pH, both during the coating [37] process as well as during filtration [46]. However, the instability at high pH can also be used as an advantage, for example in sacrificial layers [69].
PAH/PVS	3	Only a very small body of research has focused on PAH/PVS use for membranes. One paper showed that this system can be used with spin-assisted coating [70], and another demonstrated that low salt permeation rates could be obtained with this system [15].

membranes, while the results for positively terminated PEMs are found in the supporting information.

3.1. Growth and swelling of polyelectrolyte multilayer membranes on model surfaces

When studying polyelectrolyte multilayers, it is common to start by studying their growth on model surfaces. Not only does this give relevant insights into the amount of deposited material (and thus the thickness), but it also elucidates the growth mechanism. Here linear growth denotes a low mobility of both polyelectrolytes in the PEM, while exponential growth indicates mobility of at least on the adsorbing polyelectrolytes during coating [71]. Moreover, on model surfaces it is possible to determine the swelling of PEM layers by use of ellipsometry, by separately measuring the dry and wet layer thickness.

In Fig. 3a, we show the adsorption (mg/m^2) of polyelectrolyte as a function of the layer number and as measured by optical flow cell reflectometry. What is immediately apparent is that for the 9 chosen PEM systems clear differences in adsorbed amount can be observed. Indeed, after 16 layers the PAH/PAA system has an adsorbed amount 7–8 times larger than the slow growing PVA/PVS system. For PAH/PAA and PAH/PVS a clear exponential growth is observed, which for PAH/PAA is also expected from literature [37,69]. The 5 systems that contain PSS as the polyanion show very similar growth curves that seem linear but start deviating towards an exponential growth at higher bilayers numbers (Fig. S12), with PEI/PAA showing very similar behavior. The reflectometry curves are very much in line with the outcomes of ellipsometry based thickness measurements, as shown in the supporting information (Fig. S4).

In Fig. 3b we study the swelling ratio (eq. 1), and have plotted this for the 9 systems as a function of the average charge density of the used polyelectrolytes. As mentioned before, Krasemann and Tieke proposed that higher charge densities would be expected to lead to denser membranes, due to a higher density of ionic crosslinks. But the exact definition of membrane density is more complex than one would think. We feel that the most logical definition for the density of a PEM layer would be its degree of swelling. A more swollen PEM layer would allow larger distances between polymer chains and thus easier transport, while a PEM with a lower degree of swelling would be expected to function as a more selective membrane with a lower water permeability. For the systems with the lowest charge density, the polyanion is always PSS and looking at these systems, we see some evidence for a lower degree of swelling at a higher charge density, similar to other work Reurink et al. [43] However, when taking into account the other systems we see that the trend is completely broken with higher charge densities leading to an increase in swelling.

These initial measurements are thus already in direct disagreement with the hypothesis of Krasemann and Tieke. Hence, it is important to understand that discrepancy. For this it is relevant to move to similar and well understood systems, like the swelling of polyelectrolyte networks. The swelling can be described as a force balance between swelling and contracting forces. The network wants to swell due to its

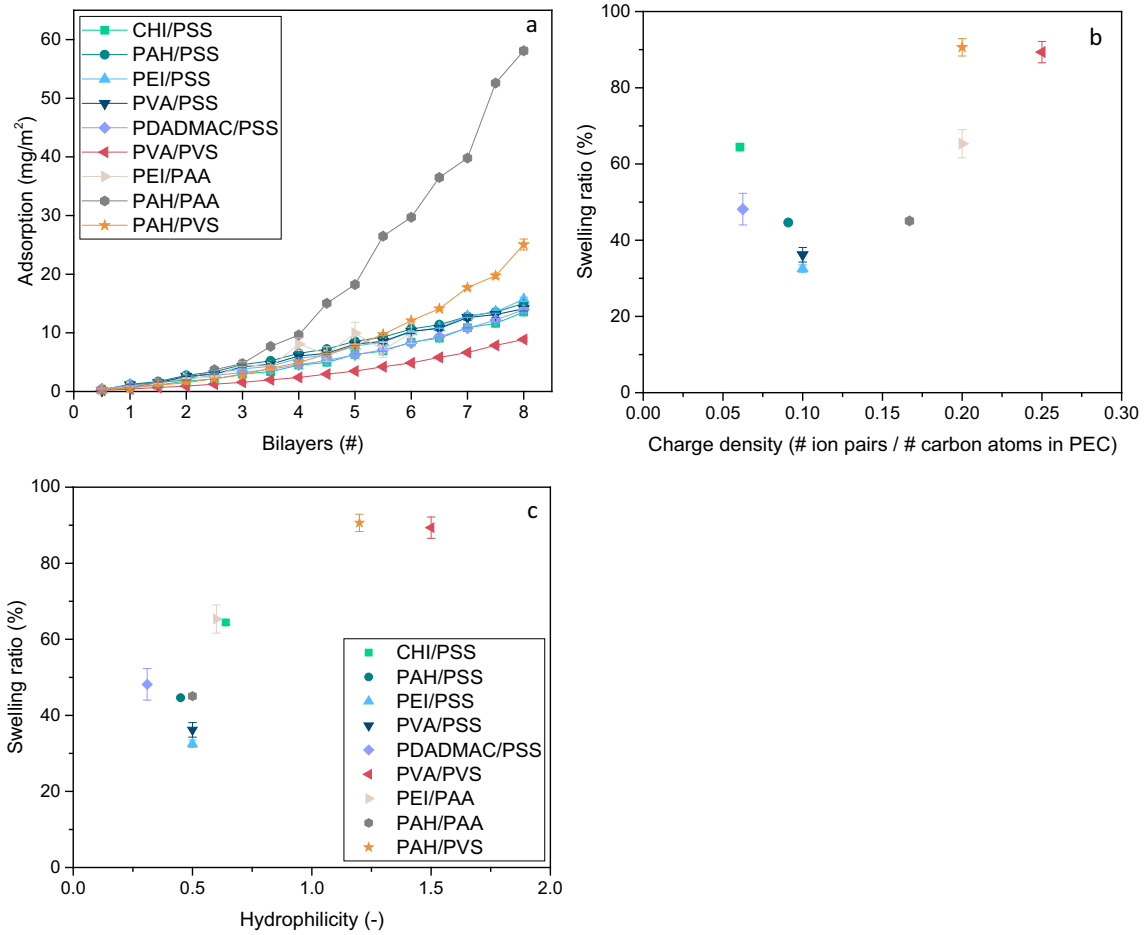

Fig. 3. a) The adsorbed amount of polyelectrolyte as a function of layer numbers for 9 different PEM systems as indicated as measured by optical reflectometry. b) the swelling of the same PEM systems as a function of charge density, the swelling was determined at 10 bilayers using ellipsometry. Here, the legend of 3a is applicable. c) The swelling ratio as a function of the hydrophilicity for all 9 different PEM systems obtained by ellipsometry. The hydrophilicity is calculated by dividing the number of heteroatoms by the amount of carbon atoms in the monomers (Table S2). Error bars indicate the standard error (n = 4).

charge, mixing entropy and affinity for the solvent, while there is an elastic counterforce connected to the entropic penalty for stretching of the polymer chains [72,73]. A higher crosslink density increases this entropic penalty, as does a higher chain flexibility. If we translate this to a PEM system, then there is a clear logic behind the hypothesis of Krasemann and Tieke, more charge density means more ionic crosslinks and thus a lower degree of swelling. However, other noncovalent interactions could influence the crosslink density as well, such as cation-π and π-π interactions in systems with PSS, and hydrogen bonding between uncharged carboxylate groups in PAA. Moreover, it is also clear that polyelectrolytes with a higher charge density will often also be more hydrophilic in nature. Such an increase in affinity between the polyelectrolytes and water would thus lead to more swelling, in line with the increase in swelling at high charge densities. If we plot swelling against the number of heteroatoms per carbon atom for each system to capture the hydrophilicity of each system somewhat better, we indeed see the same trend (Fig. 3c). Finally, one needs to keep in mind that many PEM systems are not electroneutral. Often one polyelectrolyte is present in the layer in excess, e.g. PSS/PAH where the monomer to monomer ratio has been found to be around 1:2, and a clear excess positive charge is present throughout the layer [43,74]. An excess charge would also lead to an increase in swelling by repulsion between the charged groups.

Clearly, the degree of swelling, and thus the expected density of the membrane, is not simply the result of a single parameter. Charge density and thus the degree of ionic crosslinks will be expected to have an effect, but other parameters such as polyelectrolyte hydrophilicity and the highly system specific effects of additional interactions between chemical groups and excess charge will also matter. Although it would be possible to steer towards a certain swelling degree using several parameters derived from PEM chemical structures, it would at the same time be very difficult to use these and predict an exact swelling degree. As a result, measuring the degree of swelling of a PEM on a model surface is then the easiest and exact option to obtain such information.

3.2. Layer growth and pore closure on a porous support membrane

On porous supports, PEM growth is more complicated than on a model surface. De Grooth et al. defined a layer dominated regime and a pore dominated regime, depending on the pore size of the support and the coated number of layers [35]. Initially, when coating the first layers, the membrane support pores remain open, and a layer is coated inside of the pore. With each layer, the pore becomes narrower and narrower, until the pore is filled and we enter the layer dominated regime. In this regime, every added layer now only adsorbs on top of the support membrane. Reurink et al. nuanced this picture a bit by explaining that there is always an intermediate zone, where the smallest support pores are already closed, while the biggest pores are still open [75]. In Fig. 4, we show an example of a standard approach to study the PEM layer growth on porous supports. Hollow fiber supports were coated by dip-coating, and after every coated layer a few membranes were tested to study water permeability and $MgSO_4$ retention. The quick drop in permeability between 0 and 2.5 bilayers is clear indication of pore narrowing. After 2.5 bilayers the decrease in permeability slows down while the $MgSO_4$ retention still rises quickly, here we expect to have reached the intermediate regime where more and more pores become closed off, reducing the amount of defects and allowing the retention to increase. From 5 bilayers onwards the $MgSO_4$ retention stabilizes, indicating the onset of the layer dominated regime free of defects. This onset of the layer dominated regime can be seen as the optimal coating thickness for a system, as at this number of bilayers the highest selectivity is achieved [76]. Further increasing the layer thickness does not lead to increased selectivity and only lowers the permeability. To allow a fair comparison between all the 9 PEM systems, we determined the point where pores become fully closed (see Fig. S3). In this way, all systems can be studied at their system specific optimal coating thickness.

In Fig. 5a, we compare the amount of bilayers required to achieve full

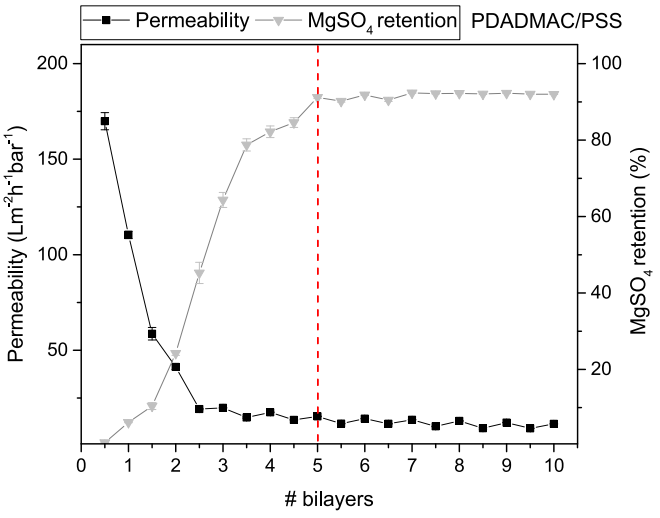

Fig. 4. A PEM membrane growth curve, where the pure water permeability and $MgSO_4$ retention are plotted against the amount of coated bilayers of PDADMAC/PSS. Error bars represent the standard error of 4 membrane experiments. These growth curves were made for all of the studied PEM systems and can be found in the supporting information (Fig. S3).

pore closure for the 9 different systems. For most systems this occurs between 5 and 9 bilayers, but there are clear outliers such as CHI/PSS with 4 bilayers and PEI/PAA with 12. Still, as shown in Fig. 3a, the growth behavior is quite system specific. A more fair way to compare the systems would be to compare the layer thickness, as estimated from ellipsometry, for which pore closure occurs. The large majority of systems has a pore closure for a layer thickness around between 10 and 20 nm, very much in line with the expected pore size of the porous support (approximately 10 nm). PAH/PAA is a system where a large thickness is found, something that is likely connected to the higher PE mobility of the system associated with its exponential growth (Fig. 3a).

With the clear optimal layer number determined for every PEM system studied in this work, it now becomes possible to fairly compare the systems for their membrane performance, this is done in the next three sections. For sake of clarity, all the permeability and retention measurements in the following sections have been performed with hollow fiber PEMMs. As indicated above, each system was coated with its optimal layer number as shown in Fig. 5a (e.g. PDADMAC/PSS – 5 bilayers, CHI/PSS – 4 bilayers, etc.). For the measurements involving model surfaces (e.g. swelling) 10 bilayers of each PEM system were coated onto a silicon wafer.

3.3. Water permeability

For any nanofiltration membrane, the (pure) water permeability is a key performance indicator as it gives information on the expected production of clean water. The water permeability would be expected to be coupled to the swelling of the membrane, with a higher swelling allowing more water molecules to permeate faster. However, water permeability is also inversely proportional to the effective thickness of the separation layer, with a thicker layer leading to more resistance and a lower water permeability.

In Fig. 6a, we plot the water permeability as a function of the charge density. Here we seem to find quite a clear trend, with a decrease in permeability as a function of charge density, although some increase is seen again at higher charge density (> 0.15). The observations seem in line with the original hypothesis of Krasemann and Tieke that at higher charge density a denser membrane is formed, and also with their observations of water transport in pervaporation [15,77].

But with the more fundamental work that we performed on model surfaces (Fig. 3) we can test this hypothesis. Already we have showed

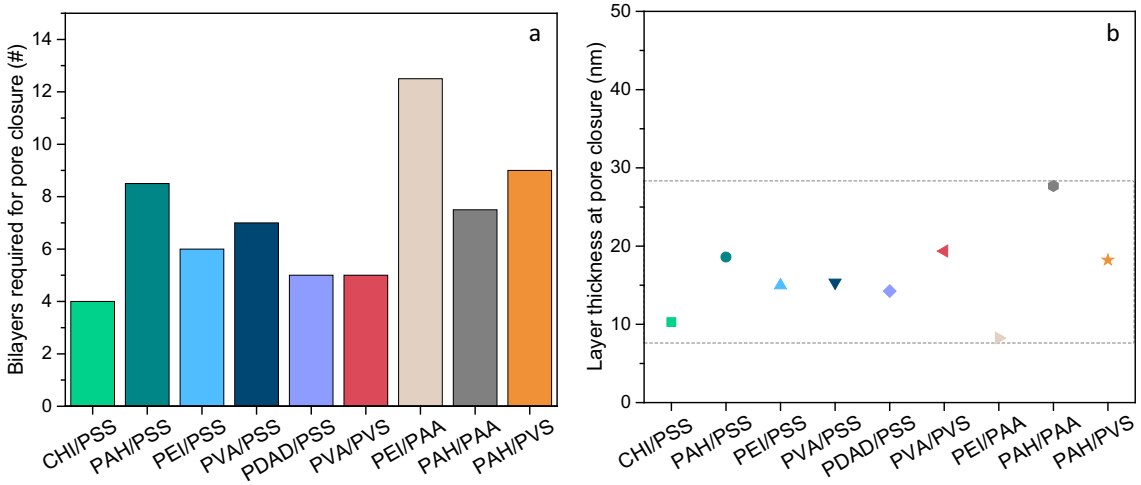

Fig. 5. a) The amount of bilayers required to fully close the support pores, as estimated from growth curves (Fig. S3). B) The corresponding layer thickness in nm, as estimated from ellipsometry data (supporting information, section S4). The swelling data stems from negatively charged polyelectrolyte multilayers.

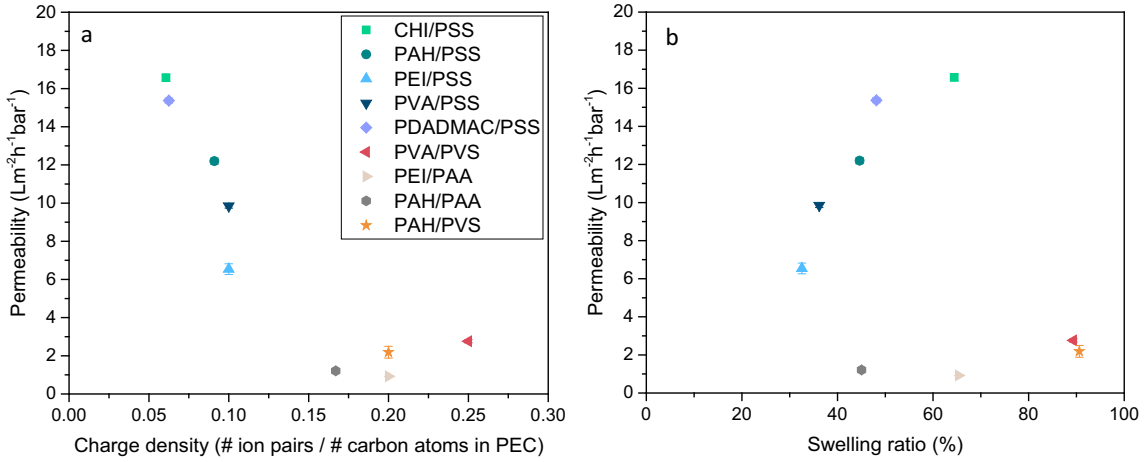

Fig. 6. Water permeability for the 9 PEM systems as plotted for the a) charge density and b) the swelling ratio. The legend displayed in Fig. 6a is for use in both Fig. 6a and b. Error bars indicate the standard error (n = 4), and are often smaller than the data markers.

that a higher charge density does not simply lead to a denser membrane with a lower degree of swelling. Plotting the swelling ratio of the PEM systems against the water permeability, as shown in Fig. 6b, we would expect a clear trend. But this is only partly true. For PEM membranes with PSS as the polyanion, a higher swelling ratio leads as expected to a higher water permeance. But for PEM systems with PAA or PVS as the anionic polyelectrolyte, relatively high swelling ratios are found, while the water permeabilities are very low. This is unexpected, as more swelling should lead to more permeability, unless there is a difference between the effective separation layer thickness. In PEM membranes, the water molecule does not just have to travel through the PEM on top of the membrane, but also through all the PEM inside of the pores. The degree or depth to which a PEM fills the membrane pores can be very different for different PEM systems. We believe that this is also the only reasonable explanation for the observations made here. Compared to the systems with PSS as the polyanion, the PEM systems that have PAA and PVS as their polyanion seem to fill the pores more efficiently, leading to much thicker separation layers, hence the low water permeabilities. This would indicate a higher chain mobility for the PVA and PAA polyanion based systems and a lower one for the PSS polyanion based systems. Indeed, we fully expect the chain mobility in the PSS polyanion systems to be lower, due to the bulky aromatic ring in PSS leading to a less flexible chain, but also to molecular interactions specifically possible in those systems including π-cation interactions between the aromatic ring and the polycation π-π interactions between PSS monomers. Also, it can be seen in Fig. 6b and Fig. 7b that the trend in PSS polyanion systems follow the same order. What stands out is that the polycations with less bulky side groups appear to have the least amount of swelling. Potentially due to stronger π- π interactions compared to the more bulky cation systems which could logically be a result from the larger distance between PSS monomers.

3.4. *The retention of neutral compounds*

For the retention of neutral compounds, the main separation mechanism will be steric hindrance, especially when the neutral compounds do not strongly interact with the separation layer. As such, a so-called molecular weight cut off (MWCO) can be determined for polyethylene glycols of different sizes, and interpreted as an effective pore size of PEM based nanofiltration membrane. These experiments were performed for all 9 systems and are reported in Fig. 7, again plotted against the charge density (Fig. 7a) and the swelling ratio (Fig. 7b).

As expected based on the results and discussion in the previous section, no correlation is observed for the MWCO as a function of the charge density. There is, however, quite a clear correlation between the MWCO and the swelling ratio of our systems, with a higher swelling also

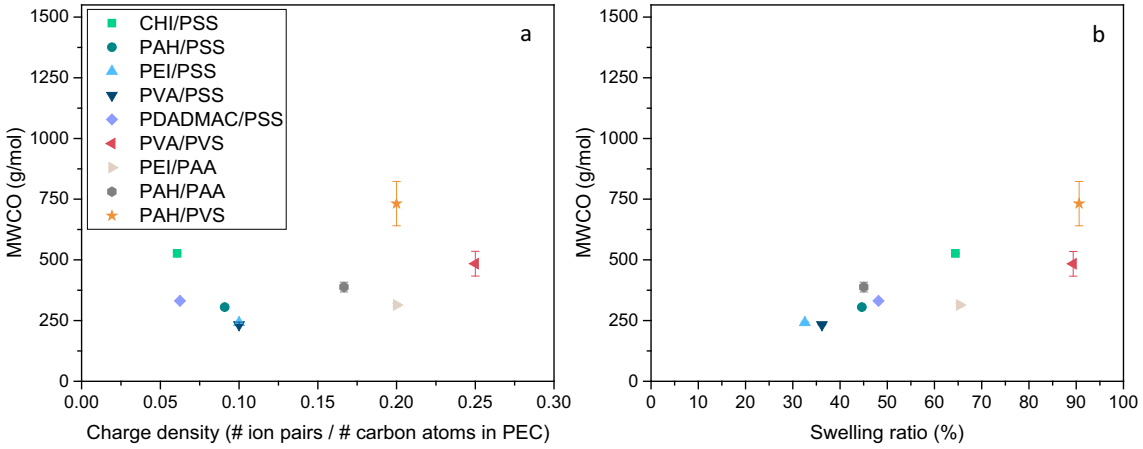

Fig. 7. MWCO for the 9 PEM systems as plotted for the a) charge density and b) the swelling ratio. Error bars indicate the standard error (n = 4) and are often smaller than the data markers. The legend of Fig. 7a also applies to Fig. 7b.

leading to a higher MWCO. Logically, for a more swollen membrane there is more distance between polymer chains and thus a lower degree of steric hindrance would be expected. Still, it is also clear that swelling is not the only parameter that matters, for example CHI/PSS and PEI/PAA have a similar swelling ratio but a quite different MWCO (around 500 and 300 respectively). We can explain this if we assume that the MWCO is determined by the mesh size of the multilayer, as originally proposed by Gresham et al. [78] The mesh size depends not only on swelling, but also crosslink density as the distance between crosslinks decreases with increasing crosslink density. A PEI/PAA system would be expected to have a small mesh size because of its very high ionic crosslink density and is only swollen so much because of the high affinity of the polyelectrolytes for water. In contrast, for CHI/PSS, the system will have lower ionic crosslink density but also less affinity for water leading to the same degree of swelling, but a larger mesh size and thus a larger MWCO.

3.5. Charged solute retention

Another key performance indicator of nanofiltration membranes is their ability to retain charged species. To characterize an NF membrane, it is especially relevant to study the retention of different salts. Here we study symmetrical salts, NaCl and $MgSO_4$, where both ions have the same valence and asymmetric salts, Na_2SO_4 and $MgCl_2$, where one ion has higher valence and will be expected to dominate the transport. As charge is key in such separation, we look at both positive and negative final layers of our PEM systems. We will first study the more straight forward case of symmetric salts, before moving to the more complex case of asymmetric salts.

We will interpret the retention of ions based on two common mechanisms, Donnan exclusion and dielectric exclusion. In Donnan exclusion, the charge on and in the separation layer will exclude similarly charged ions, while attracting oppositely charged ones. As this effect scales with the valence of the ion, it will lead to a very different separation behavior for the two asymmetric salts Na_2SO_4 and $MgCl_2$. For a negative membrane a high retention of Na_2SO_4 would be expected as there the divalent negative SO_4^{2-} is dominant, but for $MgCl_2$ a very low rejection is expected as the divalent positive Mg^{2+} dominates.

In dielectric exclusion, ions are rejected based on a difference in dielectric properties of the bulk solution and those of the separation layers. Ions prefer the high dielectric constant of water, and moving them into a separation layer with a lower dielectric constant is unfavorable, leading to retention of the ion. While this rejection mechanism also strongly depends on the valence, it is independent of the charge sign. A membrane with a high dielectric exclusion would thus show a high rejection of both Na_2SO_4 and $MgCl_2$.

3.6. Symmetric salt(s) vs. swelling ratio

When looking at the retentions of NaCl and $MgSO_4$ for both the negative and positively charge terminated PEM systems (Fig. 8) we immediately notice the large variations in retention behavior. We can go from 99 % $MgSO_4$ retention to <10 %, and from 70 % to 0 % NaCl retention. These results show very clearly the high versatility and tunability of PEM based membranes to get the specific separation properties required for an application. What we also observe is that the multivalent ions are always better retained than the monovalent ions. This is a very logical result, as both for Donnan and dielectric exclusion a higher valence would lead to more exclusion. An exception is PAH/PVS, at this point we do not have a suitable explanation for this specific outcome. In some cases this difference is quite extreme, with for example PVA/PSS (positively terminated) having a near 100 % retention of $MgSO_4$, and only a 20 % retention of NaCl. Indeed, PEM systems are seen as very relevant systems to allow separation between multivalent and monovalent salts. [34,79,80]

Here we plotted retention data against the swelling ratio of the PEM. We believe that the swelling ratio is relevant as less water in the PEM would be expected to lead to a more significant dielectric exclusion. Moreover, a higher degree of swelling could lower the effective charge density of the PEM leading to less Donnan exclusion. In general there seems to be a correlation present between swelling ratio and retention. Still, the correlation is far from perfect, as the charge density is not only determined by the degree of swelling (together with the amount of excess charge in the layer) and as the charge density of the final layer will certainly also have an effect. As discussed before these are quite system dependent and hard to predict based on the polyelectrolyte structure.

We have also plotted the retention data according to the research of Krasemann and Tieke, as a function of charge density (Fig. S7). Surprisingly we noticed that with increasing charge density, retention seemed to go down, opposite to what Krasemann and Tieke show in their work (see Fig. 1). But retention depends on water flux as well, and that was quite different, as was already shown in Fig. 6a. A more fair comparison is then to go to B values (S11), that give a flux independent permeability of salts (Fig. 9). In this case no trend is observed anymore. It should be noted that calculating the flow-independent B-value using the solution-diffusion (SD) model means that the influence of convective transport is neglected and we assume that diffusional transport is dominant. The SD model has been found to describe retention measurements as a function of flux reasonably well for similar PEM systems [48,81]. One might wonder why our results are so different from those of Krasemann and Tieke, but we stress again that there are many differences between our work. Our layers were grown under different

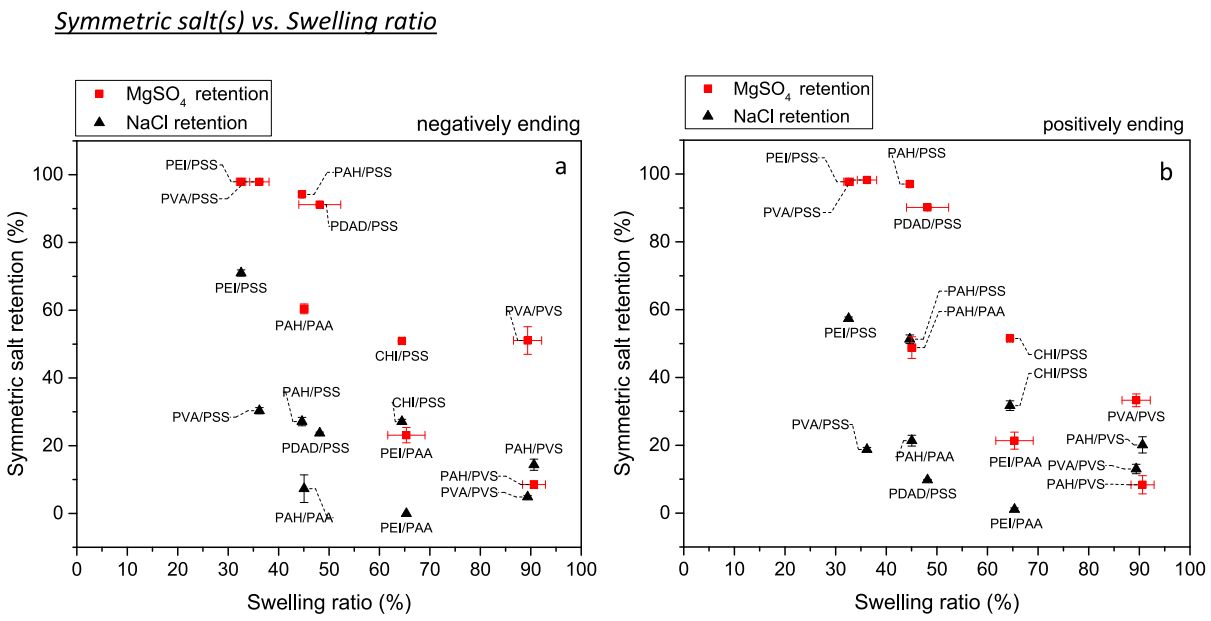

Fig. 8. The retention of NaCl and $MgSO_4$ for 9 different PEM systems as a function of the swelling ratio with a a) negatively charged final layer, and b) a positively charge final layer. Error bars indicate the standard error stemming from 4 (y-axis) and 3 (x-axis) membrane samples, and are often smaller than the data markers.

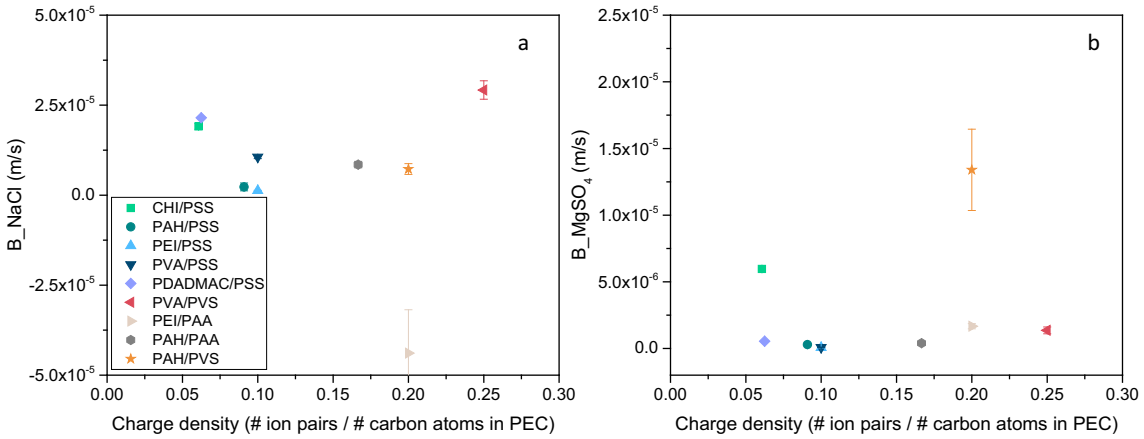

Fig. 9. The B parameter of a) NaCl and b) $MgSO_4$ for the 9 different PEM systems, plotted against the charge density. Here only the negatively terminated PEM systems are shown. The negative B-value for PEI/PAA (Fig. 9a) is the result of an experimental negative retention. Error bars indicate the standard error stemming from 4 membrane samples, and are often smaller than the data markers. The legend in Fig. 9a also applies to Fig. 9b.

conditions, and were studied under conditions relevant to nanofiltration, using applied pressure rather than studying concentration driven transport. Moreover, Krasemann and Tieke themselves already nuanced their hypothesis by mentioning the importance of pH. While in their charge density definition they assumed all monomers to carry a charge, they were well aware that for the used weak polyelectrolytes (which often have the highest charge density) the pH affects the degree of ionization. Indeed, even in PEM membranes a shift in pH can alter the excess charge in the layer from positive at lower pH values to negative at higher pH values [46,82]. Moreover, it is known that, upon incorporation into a multilayer, the pKa value of polyelectrolytes is able to shift. Resulting into a higher or lower effective pKa value and hence a different degree of ionization [83,84].

3.7. Asymmetric salt(s) vs. swelling ratio

In Fig. 10 we show the retention of our asymmetric salts, Na_2SO_4 and $MgCl_2$, again plotted as function of the degree of swelling. With these salts we can now start to differentiate between systems where the retention is more based on Donnan exclusion, and where it is more based on dielectric exclusion. For example, PAH/PSS shows a high retention of both Na_2SO_4 and $MgCl_2$, independent of the terminating layer. This is a clear indication that this system has a dominant dielectric exclusion mechanism, in line with earlier observations [43,74]. For PDADMAC/PSS, negatively terminated, we see a very large difference in retention between Na_2SO_4 and $MgCl_2$. Here a very high (99 %) retention for Na_2SO_4 is found, while for $MgCl_2$ the retention is very low (~10 %), clearly indicating a Donnan based exclusion mechanism. And certainly there are also systems where both Donnan and dielectric exclusion play a role, for example PEI/PSS where an excess negative charge in both negatively and positively terminated layers leads to more retention of Na_2SO_4, but where still a good retention of $MgCl_2$ is observed [43]. Similar behavior is seen for CHI/PSS where the retention of Na_2SO_4 is high for both negatively and positively ending layers while $MgCl_2$ retention is low, indicating an excess of negative charge independent of terminating layer. Something which has been observed for PDADMAC/PSS, where overcompensation of PDADMAC led to an excess of positive charge [60].

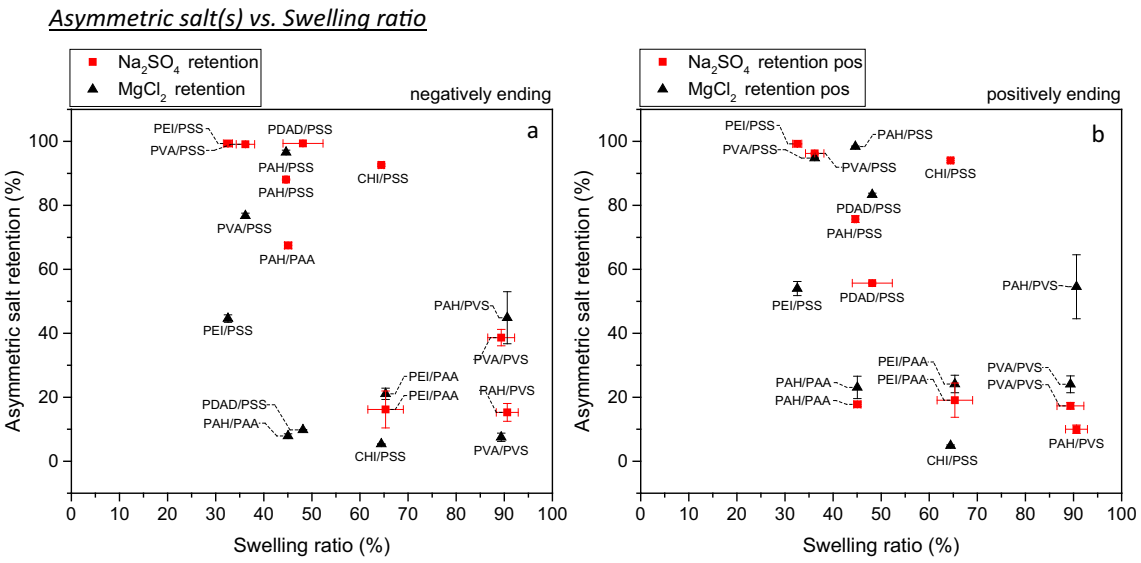

Fig. 10. The retention of Na_2SO_4 and $MgCl_2$ for 9 different PEM systems as a function of the swelling ratio with a a) negatively charged final layer, and b) a positively charged final layer. Error bars indicate the standard error stemming from 4 (y-axis) and 3 (x-axis) membrane samples, and are often smaller than the data markers.

With such variations in membrane charge and rejection mechanisms, there is no clear trend between the retention of asymmetric salts and the degree of swelling. It is the much more system specific effects such as excess charge that seem to dominate the separation behavior of these asymmetric salts. But as mentioned earlier, we would expect a correlation between swelling and especially the dielectric exclusion mechanism. One would expect that for lower water content, the dielectric constant of the PEM layer will go down and a stronger exclusion would be the result. A measure for the dielectric exclusion can be estimated by the following equation: $R_{Na2SO4} * R_{MgCl2} = DE$. This value is high when both retentions are high, but becomes low when one is high and the other is low as would be the case for Donnan exclusion. Naturally the value is also low when both retentions are low. In Fig. 11 the DE value is plotted against the swelling ratio.

Here we clearly see that high dielectric exclusion is only there for PEM layers with a low degree of swelling, around 40 %. Still, again it is much more complex that just that simple parameter, PAH/PAA with the same low swelling degree shows very little dielectric exclusion. We hypothesize that the polar nature of PAA and PAH keep the dielectric constant relatively high, even at such a low swelling ratio. In other work, however, dielectric exclusion for PAH/PAA systems has been observed [85].

For completeness we also studied the retention of Na_2SO_4 and $MgCl_2$ as a function of charge density (fig. S7). Again a trend seems to be there but can be explained by the higher fluxes at lower charge density. We then studied the more fair B parameter for these salts as shown in Fig. 12. As expected no clear trend can be observed. As mentioned above, we feel that the key parameter here is the degree of excess charge in and on the PEM, and that is simply not something that can be connected to the charge density of the used polyelectrolytes.

3.8. *From multilayer properties to membrane performance*

In the sections before we have clearly demonstrated both the versatility and the complexity of PEM based nanofiltration membranes. A wide variation of membranes can be prepared with different membrane performances, including different pure water permeabilities and different separation properties resulting from size, Donnan and

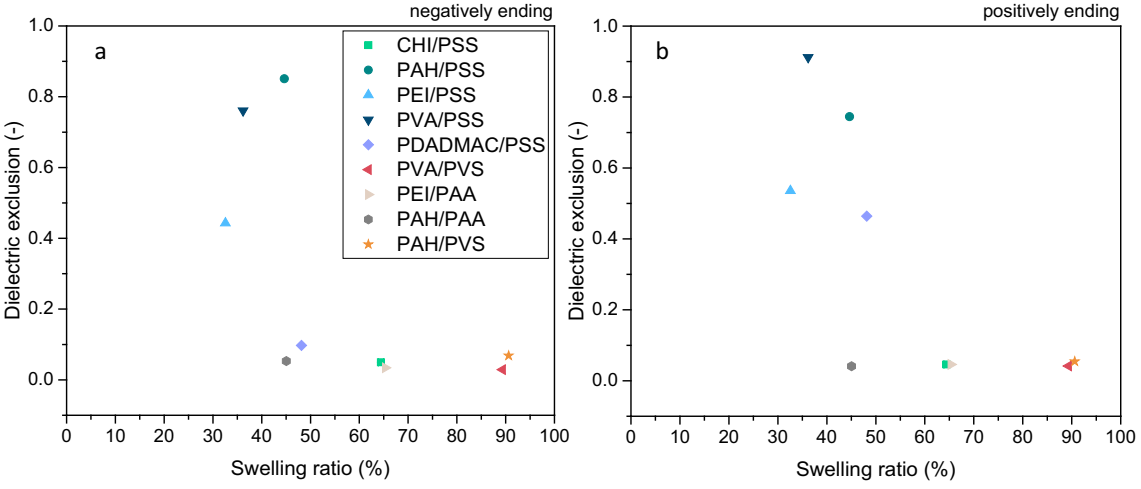

Fig. 11. The dielectric exclusion value, estimated from the retention of Na_2SO_4 and $MgCl_2$ for 9 different PEM systems as a function of the swelling ratio with a a) negatively charged final layer, and b) a positively charged final layer. Error bars indicate the standard error stemming from 3 membrane samples, and are often smaller than the data markers. The legend in Fig. 11a also applies to Fig. 11b.

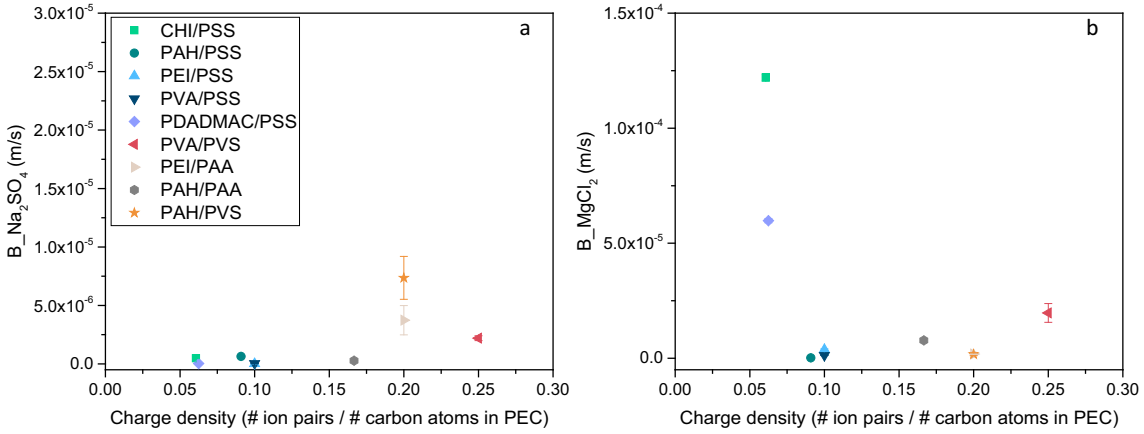

Fig. 12. The B parameter of a) Na_2SO_4 and b) $MgCl_2$ for the 9 different PEM systems, plotted against the charge density. Here only the negatively terminated PEM systems are shown. Error bars indicate the standard error stemming from 4 membrane samples, and are often smaller than the data markers. The legend in Fig. 12a also applies to Fig. 12b.

dielectric based exclusions. And here we just varied the polyelectrolyte combinations, many more PEM membrane properties become possible when also using salinity, pH, molecular weight, and other tuning parameters. But to explain these observed differences, a very wide variety of properties needed to be discussed. On one hand we have the polyelectrolyte properties, including their charge density, hydrophilicity, stiffness and naturally the nature of the charged group. We have the way that the oppositely charged polyelectrolytes interact, forming ionic crosslinks (intrinsic charge compensation) but also leaving free charged groups (extrinsic compensation). In such an ionically crosslinked network there will then also be a resulting mesh size and the polyelectrolytes often do not interact in a charge stoichiometric fashion, leading to an excess of charges in the multilayer. Moreover, there might be additional molecular interactions, for example the proposed π-cation and π-π interactions that seem to set apart PSS based PEM systems from those where the polyanion is PAA or PVS. Finally, we then have the properties of the layer itself, including the layer thickness, the final coated layer, but certainly also its degree of swelling and the degree to which the layer penetrates the pores of the membrane support. How can we now more clearly connect the properties of the multilayer to the eventual membrane performance, based on the results from our experimental review but also based on existing insights from previous works?

In Fig. 13 we show a schematic figure where we aim to clearly show what we see as the key properties of the polyelectrolyte multilayer. Moreover, in Table 2, we more clearly link these properties to the performance of the membrane, starting with the pure water permeability. As discussed in the section *water permeability*, the swelling is expected to be a key parameter for water transport. As we know that water transport in PEM membranes is mostly diffusive in nature [76], water transport would simply stem from the amount of water molecules taken up by the membrane, the speed of diffusion of these water molecules in the layer and the effective distance that the water molecules need to travel through the layer [86,87]. The degree of swelling is a direct measure for the uptake of water molecules, but in a more swollen layer the speed of diffusion of water molecules will also be higher, closer to that of bulk

Table 2
Connecting membrane performance to multilayer properties. Here we aim to define the main determining parameters, but also illustrate that these are themselves typically a result of several other parameters.

Membrane performance	Main determining PEM properties	In turn determined by
Pure water permeability	Effective layer thickness	PEM thickness on membrane Degree of pore penetration
	Degree of swelling	Ionic crosslink density Excess charge in PEM Chains hydrophilicity Chain flexibility (Kuhn length) Additional molecular interactions
Size based exclusion	PEM network mesh Size	Ionic crosslink density Degree of swelling
Donnan based exclusion	Charge density in *and on* the PEM	Excess charge in PEM Degree of swelling Final adsorbed layer
Dielectric exclusion	Dielectric constant in PEM	Degree of swelling Chains hydrophilicity Charge density in PEM

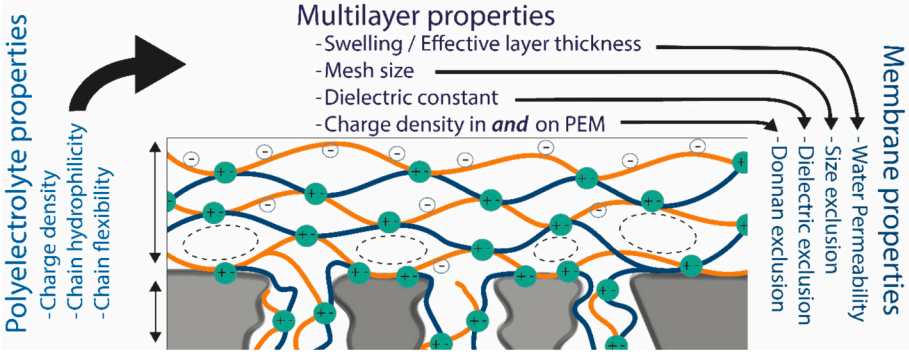

Fig. 13. Schematic representation of a PEM membrane showcasing how the most important polyelectrolyte, multilayer and membrane properties are interconnected.

water. But as shown in Fig. 6, this was not the full explanation. Even when PEMs give relatively equal layer thicknesses on top of a surface (Fig. 5b), their penetration into the membrane pores seems very dependent on the system, likely depending on chain mobility in the multilayers. It is then the PEM thickness on top of the membrane, together with the PEM in the pores that determines the effective distance that the water molecules need to travel. Hence a more swollen PEM, could still give a lower pure water permeability, due to a larger effective layer thickness. While the degree of swelling is relatively easy to measure for a PEM on a model surface, it is itself determined by many parameters, including the degree of hydrophilicity and excess charge density (that would favor swelling) and ionic crosslink density, additional attractive interchain interactions and chain flexibility (that would reduce swelling).

A similar complexity is there for the exclusion mechanisms. While there is a strong correlation between MWCO, as a measure for the size-based exclusion, and the degree of swelling (also found by Bruening et al. [45]), it does not explain the differences between all different PEM systems. As proposed by Gresham et al. [78], it is likely to be the mesh size of the PEM that functions as an effective pore size for these systems, determined by the degree of swelling together with degree of ionic crosslink density. Donnan and dielectric exclusion of a PEM would together determine the transport of (small) charged solutes but function in a different manner. For Donnan exclusion it is well established that the (excess) charge density of the separation layer is a key parameter [87,88]. For a PEM system that would include the excess charge in the membrane, which together with the degree of swelling determines that layer charge density, but certainly also the charge at the outer layer that is in large part determined by the choice of the final adsorbed layer [35]. Finally the solution pH will affect the excess charge density when weak polyelectrolytes are part of the PEM based membrane [46,82]. For dielectric exclusion it is the dielectric constant of the layer that would determine the rejection properties, but in our review a dominant dielectric exclusion mechanism is only found when the degree of swelling is sufficiently low (Fig. 11). That is not strange, the lower the degree of swelling, the lower the dielectric constant of a polymer layer will be. It is still expected that also the hydrophilicity of the layer will affect the dielectric properties, as well as the charge density in the layer as the latter will attract counterions and will orient the water molecules, however this is speculative and not something that came directly out of the experimental review provided here.

While Fig. 13 and Table 2 paint a rather complex picture of PEMs and their separation behavior, we want to again make the argument that this is to be expected for such a versatile system. Clearly, the initial explanation of Tieke and Krasemann, coupling chain charge density to the "openness" of the formed multilayer, had a lot of scientific merit, helping the field forward. However, we now need to also realize that there is no easy single parameter that determines the PEM membrane performance, it is a rather complex interplay resulting from various parameters. But this is at the same time also a real strength, it is exactly this complexity that allows one to optimize a PEM towards a specific application by tuning multiple parameters. For example, this has already allowed the creation of PEM membranes with dominant Donnan or dielectric behavior, or rather a combination of the two, as seen in this work and in many others. Or the creation of PEM based membranes with a high degree of size exclusion (low MWCO) and low salt retentions [55], or inversely, very open PEMs (high MWCO) with high salt retentions [2].

4. Conclusions

One of the core strengths of polyelectrolyte multilayer membranes is their high versatility. By tuning parameters such as pH and salinity during coating, the membranes can be optimized for specific applications. But this also makes a fair comparison between different PEM systems difficult, in literature systems are nearly always prepared in a different manner, and/or measured under different process conditions. In this work we have performed an experimental review, where 9 common PEM based systems were prepared and characterized under very controlled and comparable conditions.

From the onset of this work we compare our results to one of the earliest papers on PEM based membranes, the work of Krasemann and Tieke [15]. While they were one of the first, to our knowledge they are also the only ones before us to have carefully studied many different PEM couples and to look for correlations in their behavior. Based on their results they proposed that the charge density of the polyelectrolytes is the key parameter, a higher charge density leading to more ionic crosslinks and thus a denser membrane. We tested this hypothesis by measuring the swelling degree for the 9 different systems, where the swelling degree is a direct measure for how open or dense a membrane is. While we find some correlation for the PEM systems based on the polyanion PSS, the overall results clearly show that the hypothesis is too limited. Indeed, other parameters such as the hydrophilicity of the used polyelectrolytes and excess charge in the layer will also influence the swelling. Due to this complexity, it becomes more straightforward to measure the degree of swelling, rather than predicting it from molecular properties.

Rather than defining a single main parameter that affects the separation properties of a PEM, we show clearly that membrane performance can be connected to the PEM layer properties through detailed experimental characterization and by separately looking at the exclusion mechanisms (see Fig. 13 and Table 2). For example, our work demonstrates a very clear correlation between MWCO and the degree of swelling. Another important outcome of our work relates to the balance between Donnan and Di-electric exclusion as observed from our ion-retentions. Especially around and below a 40 % swelling degree, strong effects of dielectric exclusion are found. On the other hand, for systems with a degree of swelling higher than 40 % clear examples of Donnan dominated exclusion are observed. These outcomes give clear directions on how to obtain desired rejection of neutral and charged molecules. Also, we demonstrate that the porous support membrane is closed by a PEM, when the thickness is in the order of the membrane support pore size. Something that has not been demonstrated before, however does need further investigation as this potentially has major influence on overall PEM properties.

Overall this experimental review shows again how versatile PEM based membranes are, with a wide variation in separation properties observed between the systems. Unfortunately, there is no single predictive parameter that connects the chemical structure of the used polyelectrolytes to their performance. Rather this work highlights several key parameters that can be obtained by careful characterization of the layers. Of these, especially the degree of swelling is critical as it partly determines the water permeability, but also partly the size exclusion, Donnan exclusion and dielectric exclusion properties. Swelling, in turn, can be related to polyelectrolyte charge density, chain flexibility and hydrophilicity, but also to the ionic crosslink density in the PEM. We strongly feel that this more nuanced look at PEM based membranes is critical to push this field forward. By careful characterization of PEMs on model surfaces and coupling the results to detailed transport measurements, much progress can still be made to further tune and improve these now established membrane systems.

CRediT authorship contribution statement

Jurjen A. Regenspurg: Writing – original draft, Methodology, Investigation, Formal analysis, Conceptualization. **Wendy A. Jonkers:** Writing – review & editing, Writing – original draft, Investigation, Formal analysis. **Moritz A. Junker:** Writing – review & editing, Methodology, Investigation, Conceptualization. **Iske Achterhuis:** Methodology, Investigation, Formal analysis, Conceptualization. **Esra te Brinke:** Writing – review & editing, Supervision, Methodology, Investigation, Conceptualization. **Wiebe M. de Vos:** Writing – review &

editing, Writing – original draft, Supervision, Funding acquisition, Conceptualization.

Declaration of competing interest

The authors declare the following financial interests/personal relationships which may be considered as potential competing interests: Wiebe M. de Vos reports financial support was provided by Nederlandse Organisatie voor Wetenschappelijk Onderzoek Utrecht. If there are other authors, they declare that they have no known competing financial interests or personal relationships that could have appeared to influence the work reported in this paper.

Acknowledgements

The authors would like to thank Viatcheslav (Slava) Freger for his kind advice and ideas with regard to Fig. 11 and the dielectric exclusion parameter. Furthermore, the authors thank Dennis Reurink and Tao Wang for their help with performing crossflow and reflectometry experiments. Lastly, the authors want to acknowledge NX Filtration B.V., Enschede, the Netherlands for kindly providing us with modified poly (ethersulfone) HF UF membranes. Funding was obtain through the Dutch science foundation (NWO) through LIFT grant 731.016.404 and NWO-TTW grant 17744.

Appendix A. Supplementary data

Supplementary data to this article can be found online at https://doi.org/10.1016/j.desal.2024.117693.

References

[1] G. Decher, J.-D. Hong, Buildup of ultrathin multilayer films by a self-assembly process, 1 consecutive adsorption of anionic and cationic bipolar amphiphiles on charged surfaces, Makromol. Chem. Macromol. Symp. 46 (1) (1991) 321–327.
[2] W.A. Jonkers, E.R. Cornelissen, W.M. de Vos, Hollow fiber nanofiltration: from lab-scale research to full-scale applications, J. Membr. Sci. 669 (2023) 121234.
[3] S.T. Dubas, J.B. Schlenoff, Factors controlling the growth of polyelectrolyte multilayers, Macromolecules 32 (24) (1999) 8153–8160.
[4] M. Lösche, J. Schmitt, G. Decher, W.G. Bouwman, K. Kjaer, Detailed structure of molecularly thin polyelectrolyte multilayer films on solid substrates as revealed by neutron reflectometry, Macromolecules 31 (25) (1998) 8893–8906.
[5] N.G. Hoogeveen, M.A. Cohen Stuart, G.J. Fleer, M.R. Böhmer, Formation and stability of multilayers of polyelectrolytes, Langmuir 12 (15) (1996) 3675–3681.
[6] K. Lowack, C.A. Helm, Molecular mechanisms controlling the self-assembly process of polyelectrolyte multilayers, Macromolecules 31 (3) (1998) 823–833.
[7] E.R. Kleinfeld, G.S. Ferguson, Stepwise formation of multilayered nanostructural films from macromolecular precursors, Science 265 (5170) (1994) 370–373.
[8] Y. Lvov, K. Ariga, I. Ichinose, T. Kunitake, Assembly of multicomponent protein films by means of electrostatic layer-by-layer adsorption, J. Am. Chem. Soc. 117 (22) (1995) 6117–6123.
[9] V.V. Tsukruk, F. Rinderspacher, V.N. Bliznyuk, Self-assembled multilayer films from dendrimers, Langmuir 13 (8) (1997) 2171–2176.
[10] G. Decher, B. Lehr, K. Lowack, Y. Lvov, J. Schmitt, New nanocomposite films for biosensors: layer-by-layer adsorbed films of polyelectrolytes, proteins or DNA, Biosens. Bioelectron. 9 (9) (1994) 677–684.
[11] F. Caruso, R.A. Caruso, H. Möhwald, Nanoengineering of inorganic and hybrid hollow spheres by colloidal templating, Science 282 (5391) (1998) 1111–1114.
[12] X. Yang, S. Johnson, J. Shi, T. Holesinger, B. Swanson, Polyelectrolyte and molecular host ion self-assembly to multilayer thin films: an approach to thin film chemical sensors, Sensors Actuators B Chem. 45 (2) (1997) 87–92.
[13] M. Müller, T. Rieser, K. Lunkwitz, J. Meier-Haack, Polyelectrolyte complex layers: a promising concept for anti-fouling coatings verified by in-situ ATR-FTIR spectroscopy, Macromol. Rapid Commun. 20 (12) (1999) 607–611.
[14] F. van Ackern, L. Krasemann, B. Tieke, Ultrathin membranes for gas separation and pervaporation prepared upon electrostatic self-assembly of polyelectrolytes, Thin Solid Films 327-329 (1998) 762–766.
[15] L. Krasemann, B. Tieke, Selective ion transport across self-assembled alternating multilayers of cationic and anionic polyelectrolytes, Langmuir 16 (2) (2000) 287–290.
[16] J.J. Harris, J.L. Stair, M.L. Bruening, Layered polyelectrolyte films as selective, ultrathin barriers for anion transport, Chem. Mater. 12 (7) (2000) 1941–1946.
[17] J. Dai, G.L. Baker, M.L. Bruening, Use of porous membranes modified with polyelectrolyte multilayers as substrates for protein arrays with low nonspecific adsorption, Anal. Chem. 78 (1) (2006) 135–140.
[18] V. Smuleac, D.A. Butterfield, D. Bhattacharyya, Layer-by-layer-assembled microfiltration membranes for biomolecule immobilization and enzymatic catalysis, Langmuir 22 (24) (2006) 10118–10124.
[19] U.K. Aravind, J. Mathew, C.T. Aravindakumar, Transport studies of BSA, lysozyme and ovalbumin through chitosan/polystyrene sulfonate multilayer membrane, J. Membr. Sci. 299 (1) (2007) 146–155.
[20] B.W. Stanton, J.J. Harris, M.D. Miller, M.L. Bruening, Ultrathin, multilayered polyelectrolyte films as nanofiltration membranes, Langmuir 19 (17) (2003) 7038–7042.
[21] A. Toutianoush, W. Jin, H. Deligöz, B. Tieke, Polyelectrolyte multilayer membranes for desalination of aqueous salt solutions and seawater under reverse osmosis conditions, Appl. Surf. Sci. 246 (4) (2005) 437–443.
[22] S. Mulyati, R. Takagi, A. Fujii, Y. Ohmukai, H. Matsuyama, Simultaneous improvement of the monovalent anion selectivity and antifouling properties of an anion exchange membrane in an electrodialysis process, using polyelectrolyte multilayer deposition, J. Membr. Sci. 431 (2013) 113–120.
[23] C. Cheng, N. White, H. Shi, M. Robson, M.L. Bruening, Cation separations in electrodialysis through membranes coated with polyelectrolyte multilayers, Polymer 55 (6) (2014) 1397–1403.
[24] J. de Grooth, D.M. Reurink, J. Ploegmakers, W.M. de Vos, K. Nijmeijer, Charged micropollutant removal with hollow fiber nanofiltration membranes based on polycation/polyzwitterion/polyanion multilayers, ACS Appl. Mater. Interfaces 6 (19) (2014) 17009–17017.
[25] D. Menne, J. Kamp, J. Erik Wong, M. Wessling, Precise tuning of salt retention of backwashable polyelectrolyte multilayer hollow fiber nanofiltration membranes, J. Membr. Sci. 499 (2016) 396–405.
[26] G. Zhang, X. Song, S. Ji, N. Wang, Z. Liu, Self-assembly of inner skin hollow fiber polyelectrolyte multilayer membranes by a dynamic negative pressure layer-by-layer technique, J. Membr. Sci. 325 (1) (2008) 109–116.
[27] S. Rajabzadeh, C. Liu, L. Shi, R. Wang, Preparation of low-pressure water softening hollow fiber membranes by polyelectrolyte deposition with two bilayers, Desalination 344 (2014) 64–70.
[28] T. Ormanci-Acar, M. Mohammadifakhr, N.E. Benes, W.M. de Vos, Defect free hollow fiber reverse osmosis membranes by combining layer-by-layer and interfacial polymerization, J. Membr. Sci. 610 (2020) 118277.
[29] J. de Grooth, B. Haakmeester, C. Wever, J. Potreck, W.M. de Vos, K. Nijmeijer, Long term physical and chemical stability of polyelectrolyte multilayer membranes, J. Membr. Sci. 489 (2015) 153–159.
[30] K. Remmen, B. Müller, J. Köser, M. Wessling, T. Wintgens, Phosphorus recovery in an acidic environment using layer-by-layer modified membranes, J. Membr. Sci. 582 (2019) 254–263.
[31] M.G. Elshof, W.M. de Vos, J. de Grooth, N.E. Benes, On the long-term pH stability of polyelectrolyte multilayer nanofiltration membranes, J. Membr. Sci. 615 (2020) 118532.
[32] T. Sewerin, M.G. Elshof, S. Matencio, M. Boerrigter, J. Yu, J. de Grooth, Advances and applications of hollow fiber nanofiltration membranes: a review, Membranes 11 (11) (2021) 890.
[33] X. Li, C. Liu, B. Van der Bruggen, Polyelectrolytes self-assembly: versatile membrane fabrication strategy, J. Mater. Chem. A 8 (40) (2020) 20870–20896.
[34] E.N. Durmaz, S. Sahin, E. Virga, S. de Beer, L.C.P.M. de Smet, W.M. de Vos, Polyelectrolytes as building blocks for next-generation membranes with advanced functionalities, ACS Applied Polymer Materials 3 (9) (2021) 4347–4374.
[35] J. de Grooth, R. Oborný, J. Potreck, K. Nijmeijer, W.M. de Vos, The role of ionic strength and odd–even effects on the properties of polyelectrolyte multilayer nanofiltration membranes, J. Membr. Sci. 475 (2015) 311–319.
[36] A. Casimiro, C. Weijers, D. Scheepers, Z. Borneman, K. Nijmeijer, Kosmotropes and chaotropes: specific ion effects to tailor layer-by-layer membrane characteristics and performances, J. Membr. Sci. 672 (2023) 121446.
[37] S. Ilyas, S.M. Abtahi, N. Akkilic, H.D.W. Roesink, W.M. de Vos, Weak polyelectrolyte multilayers as tunable separation layers for micro-pollutant removal by hollow fiber nanofiltration membranes, J. Membr. Sci. 537 (2017) 220–228.
[38] J.A. Regenspurg, A.F. Martins Costa, I. Achterhuis, W.M. de Vos, Influence of molecular weight on the performance of polyelectrolyte multilayer nanofiltration membranes, ACS Applied Polymer Materials 4 (5) (2022) 2962–2971.
[39] M.D. Miller, M.L. Bruening, Controlling the nanofiltration properties of multilayer polyelectrolyte membranes through variation of film composition, Langmuir 20 (26) (2004) 11545–11551.
[40] J. Luo, C. Dong, R. He, C. Liu, T. He, Impact of support pore properties on the performance of layer-by-layer self-assembly nanofiltration membrane, Desalination 557 (2023) 116596.
[41] D.M. Reurink, J.P. Haven, I. Achterhuis, S. Lindhoud, H.D.W. Roesink, W.M. de Vos, Annealing of polyelectrolyte multilayers for control over ion permeation, Adv. Mater. Interfaces 5 (20) (2018) 1800651.
[42] K.L. Cho, A.J. Hill, F. Caruso, S.E. Kentish, Membranes: chlorine resistant glutaraldehyde crosslinked polyelectrolyte multilayer membranes for desalination (Adv. Mater. 17/2015), Adv. Mater. 27 (17) (2015) 2811.
[43] D.M. Reurink, J.D. Willott, H.D.W. Roesink, W.M. de Vos, Role of polycation and cross-linking in polyelectrolyte multilayer membranes, ACS Applied Polymer Materials 2 (11) (2020) 5278–5289.
[44] D. Scheepers, A. Casimiro, Z. Borneman, K. Nijmeijer, Addressing specific (poly)ion effects for layer-by-layer membranes, ACS Applied Polymer Materials 5 (3) (2023) 2032–2042.
[45] M.D. Miller, M.L. Bruening, Correlation of the swelling and permeability of polyelectrolyte multilayer films, Chem. Mater. 17 (21) (2005) 5375–5381.

[46] M.A. Junker, J.A. Regenspurg, C.I. Valdes Rivera, E.t Brinke, W.M. de Vos, Effects of feed solution pH on polyelectrolyte multilayer nanofiltration membranes, ACS Applied Polymer Materials 5 (1) (2023) 355–369.
[47] J.C. Dijt, M.A.C. Stuart, J.E. Hofman, G.J. Fleer, Kinetics of polymer adsorption in stagnation point flow, Colloids Surf. A Physicochem. Eng. Asp. 51 (1990) 141–158.
[48] M.A. Junker, W.M. de Vos, R.G.H. Lammertink, J. de Grooth, Bridging the gap between lab-scale and commercial dimensions of hollow fiber nanofiltration membranes, J. Membr. Sci. 624 (2021) 119100.
[49] W. Ritcharoen, P. Supaphol, P. Pavasant, Development of polyelectrolyte multilayer-coated electrospun cellulose acetate fiber mat as composite membranes, Eur. Polym. J. 44 (12) (2008) 3963–3968.
[50] J. Mathew, A. Gopalakrishnan, C.T. Aravindakumar, U.K. Aravind, Transport properties and morphology of CHI/PSS multilayered microfiltration membranes for the low pressure filtration of amino acids, J. Chem. Technol. Biotechnol. 92 (4) (2017) 834–844.
[51] U.K. Aravind, B. George, M.S. Baburaj, S. Thomas, A.P. Thomas, C. T. Aravindakumar, Treatment of industrial effluents using polyelectrolyte membranes, Desalination 252 (1) (2010) 27–32.
[52] W. Jin, A. Toutianoush, B. Tieke, Size- and charge-selective transport of aromatic compounds across polyelectrolyte multilayer membranes, Appl. Surf. Sci. 246 (4) (2005) 444–450.
[53] S.U. Hong, R. Malaisamy, M.L. Bruening, Optimization of flux and selectivity in Cl−/SO42− separations with multilayer polyelectrolyte membranes, J. Membr. Sci. 283 (1) (2006) 366–372.
[54] X. Liu, M.L. Bruening, Size-selective transport of uncharged solutes through multilayer polyelectrolyte membranes, Chem. Mater. 16 (2) (2004) 351–357.
[55] E. te Brinke, D.M. Reurink, I. Achterhuis, J. de Grooth, W.M. de Vos, Asymmetric polyelectrolyte multilayer membranes with ultrathin separation layers for highly efficient micropollutant removal, Appl. Mater. Today 18 (2020) 100471.
[56] E. te Brinke, I. Achterhuis, D.M. Reurink, J. de Grooth, W.M. de Vos, Multiple approaches to the buildup of asymmetric polyelectrolyte multilayer membranes for efficient water purification, ACS Applied Polymer Materials 2 (2) (2020) 715–724.
[57] A.M. Alghamdi, Fast and versatile pathway in fabrication of polyelectrolyte multilayer nanofiltration membrane with tunable properties, J. Chemother. 2021 (2021) 9978596.
[58] C. Wang, M.J. Park, D.H. Seo, S. Phuntsho, R.R. Gonzales, H. Matsuyama, E. Drioli, H.K. Shon, Inkjet printed polyelectrolyte multilayer membrane using a polyketone support for organic solvent nanofiltration, J. Membr. Sci. 642 (2022) 119943.
[59] A. Toutianoush, J. Schnepf, A. El Hashani, B. Tieke, Selective ion transport and complexation in layer-by-layer assemblies of p-sulfonato- calix[n]arenes and cationic polyelectrolytes, Adv. Funct. Mater. 15 (4) (2005) 700–708.
[60] R.A. Ghostine, M.Z. Markarian, J.B. Schlenoff, Asymmetric growth in polyelectrolyte multilayers, J. Am. Chem. Soc. 135 (20) (2013) 7636–7646.
[61] A. Toutianoush, B. Tieke, Selective transport and incorporation of highly charged metal and metal complex ions in self-assembled polyelectrolyte multilayer membranes, Mater. Sci. Eng. C 22 (2) (2002) 135–139.
[62] L. Krasemann, A. Toutianoush, B. Tieke, Self-assembled polyelectrolyte multilayer membranes with highly improved pervaporation separation of ethanol/water mixtures, J. Membr. Sci. 181 (2) (2001) 221–228.
[63] A. Toutianoush, L. Krasemann, B. Tieke, Polyelectrolyte multilayer membranes for pervaporation separation of alcohol/water mixtures, Colloids Surf. A Physicochem. Eng. Asp. 198-200 (2002) 881–889.
[64] A. Toutianoush, B. Tieke, Pervaporation separation of alcohol/water mixtures using self-assembled polyelectrolyte multilayer membranes of high charge density, Mater. Sci. Eng. C 22 (2) (2002) 459–463.
[65] G. Zhang, W. Gu, S. Ji, Z. Liu, Y. Peng, Z. Wang, Preparation of polyelectrolyte multilayer membranes by dynamic layer-by-layer process for pervaporation separation of alcohol/water mixtures, J. Membr. Sci. 280 (1) (2006) 727–733.
[66] Y.-H. Yang, M. Haile, Y.T. Park, F.A. Malek, J.C. Grunlan, Super gas barrier of all-polymer multilayer thin films, Macromolecules 44 (6) (2011) 1450–1459.
[67] N. Dizge, R. Epsztein, W. Cheng, C.J. Porter, M. Elimelech, Biocatalytic and salt selective multilayer polyelectrolyte nanofiltration membrane, J. Membr. Sci. 549 (2018) 357–365.
[68] Y. Liu, G.Q. Chen, X. Yang, H. Deng, Preparation of layer-by-layer nanofiltration membranes by dynamic deposition and crosslinking, Membranes 9 (2) (2019) 20.
[69] S. Ilyas, J. de Grooth, K. Nijmeijer, W.M. de Vos, Multifunctional polyelectrolyte multilayers as nanofiltration membranes and as sacrificial layers for easy membrane cleaning, J. Colloid Interface Sci. 446 (2015) 386–393.
[70] F. Fadhillah, S.M. Javaid Zaidi, Z. Khan, M. Khaled, F. Rahman, P. Hammond, Development of multilayer polyelectrolyte thin-film membranes fabricated by spin assisted layer-by-layer assembly, J. Appl. Polym. Sci. 126 (4) (2012) 1468–1474.
[71] P. Lavalle, C. Gergely, F.J.G. Cuisinier, G. Decher, P. Schaaf, J.C. Voegel, C. Picart, Comparison of the structure of polyelectrolyte multilayer films exhibiting a linear and an exponential growth regime: an in situ atomic force microscopy study, Macromolecules 35 (11) (2002) 4458–4465.
[72] F. Horkay, G.B. McKenna, Polymer networks and gels, in: M.E. James (Ed.), Physical Properties of Polymers Handbook vol. 2, Springer, New York, NY, 2007, pp. 497–523.
[73] P.J. Flory, J. Rehner Jr., Statistical mechanics of cross-linked polymer networks II. Swelling, J. Chem. Phys. 11 (11) (2004) 521–526.
[74] J. Kamp, S. Emonds, M. Wessling, Designing tubular composite membranes of polyelectrolyte multilayer on ceramic supports with nanofiltration and reverse osmosis transport properties, J. Membr. Sci. 620 (2021) 118851.
[75] D.M. Reurink, F. Du, R. Górecki, H.D.W. Roesink, W.M. de Vos, Aquaporin-containing proteopolymersomes in polyelectrolyte multilayer membranes, Membranes 10 (5) (2020) 103.
[76] M.A. Junker, W.M. de Vos, J. de Grooth, R.G.H. Lammertink, Relating uncharged solute retention of polyelectrolyte multilayer nanofiltration membranes to effective structural properties, J. Membr. Sci. 668 (2023) 121164.
[77] L. Krasemann, B. Tieke, Composite membranes with ultrathin separation layer prepared by self-assembly of polyelectrolytes, Mater. Sci. Eng. C 8-9 (1999) 513–518.
[78] I.J. Gresham, D.M. Reurink, S.W. Prescott, A.R.J. Nelson, W.M. de Vos, J.D. Willott, Structure and hydration of asymmetric polyelectrolyte multilayers as studied by neutron reflectometry: connecting multilayer structure to superior membrane performance, Macromolecules 53 (23) (2020) 10644–10654.
[79] W. Cheng, C. Liu, T. Tong, R. Epsztein, M. Sun, R. Verduzco, J. Ma, M. Elimelech, Selective removal of divalent cations by polyelectrolyte multilayer nanofiltration membrane: role of polyelectrolyte charge, ion size, and ionic strength, J. Membr. Sci. 559 (2018) 98–106.
[80] R. He, C. Dong, S. Xu, C. Liu, S. Zhao, T. He, Unprecedented Mg2+/Li+ separation using layer-by-layer based nanofiltration hollow fiber membranes, Desalination 525 (2022) 115492.
[81] W.A. Jonkers, W.M. de Vos, E. te Brinke, Asymmetric polyelectrolyte multilayer membranes: influence of bottom section polycation on layer growth and retention mechanisms, J. Membr. Sci. 698 (2024) 122577.
[82] M. Ahmad, A. Yaroshchuk, M.L. Bruening, Moderate pH changes alter the fluxes, selectivities and limiting currents in ion transport through polyelectrolyte multilayers deposited on membranes, J. Membr. Sci. 616 (2020) 118570.
[83] H.H. Rmaile, J.B. Schlenoff, “Internal pKa’s” in polyelectrolyte multilayers: coupling protons and salt, Langmuir 18 (22) (2002) 8263–8265.
[84] J.D. Mendelsohn, C.J. Barrett, V.V. Chan, A.J. Pal, A.M. Mayes, M.F. Rubner, Fabrication of microporous thin films from polyelectrolyte multilayers, Langmuir 16 (11) (2000) 5017–5023.
[85] M.A. Junker, E. te Brinke, C.M. Vall Compte, R.G.H. Lammertink, J. de Grooth, W. M. de Vos, Asymmetric polyelectrolyte multilayer nanofiltration membranes: structural characterisation via transport phenomena, J. Membr. Sci. 681 (2023) 121718.
[86] R.W. Baker, Membrane transport theory, in: Membrane Technology and Applications, 3ed, John Wiley and Sons Ltd, United Kingdom, 2012, pp. 15–96.
[87] M. Mulder, Transport in membranes, in: Basic Principles of Membrane Technology, 2 ed, Kluwer Academic Publishers, the Netherlands, 1996, pp. 210–271.
[88] R.W. Baker, Ion exchange membrane processes - electrodialysis, in: Membrane Technology and Applications, 3ed, John Wiley and Sons Ltd, United Kingdom, 2012, pp. 417–452.